THE FASEB JOURNAL • RESEARCH • www.fasebj.org

Deposition of microparticles by neutrophils onto inflamed epithelium: a new mechanism to disrupt epithelial intercellular adhesions and promote transepithelial migration

Veronika Butin-Israeli,* Madelyn C. Houser,† Mingli Feng,‡ Edward B. Thorp,* Asma Nusrat,‡ Charles A. Parkos,‡ and Ronen Sumagin*,[1]

*Department of Pathology, Feinberg School of Medicine, Northwestern University, Chicago, Illinois, USA; †Department of Physiology, Emory University School of Medicine, Atlanta, Georgia, USA; and, ‡Department of Pathology, University of Michigan Medical School, Ann Arbor, Michigan, USA

ABSTRACT: Neutrophil [polymorphonuclear leukocyte (PMN)] transepithelial migration (TEM) is a hallmark of inflammatory mucosal disorders. PMN TEM is associated with epithelial injury; however, mechanisms involved in this process are not well defined. The current work describes a new mechanism whereby deposition of PMN membrane-derived microparticles (PMN-MPs) onto intestinal epithelial cells (IECs) during TEM leads to loss of epithelial cadherins, thus promoting epithelial injury and increased PMN recruitment. PMN-MPs secreted by activated PMNs during TEM displayed a high level of enzymatically active matrix metalloproteinase 9 (MMP-9), and were capable of mediating potent effects on IEC integrity. Isolated PMN-MPs efficiently bound to IEC monolayers and induced cleavage of desmoglein-2 (DSG-2) but not E-cadherin, leading to disruption of IEC intercellular adhesions. Furthermore, PMN-MP binding to intestinal epithelium *in vitro* in transwell assays and *in vivo* in ligated intestinal loop preparations facilitated increases in PMN TEM. These effects were MMP-9 dependent and were reversed in the presence of specific pharmacological inhibitors. Finally, we demonstrated that IEC Dsg-2 serves as a barrier for migrating PMNs, and its removal by PMN-MP-associated MMP-9 facilitates PMN trafficking across epithelial layers. Our findings thus implicate PMN-MPs in PMN-mediated inflammation and epithelial damage, as observed in inflammatory disorders of mucosal surfaces.—Butin-Israeli, V., Houser, M. C., Feng, M., Thorp, E. B., Nusrat, A., Parkos, C. A, Sumagin, R. Deposition of microparticles by neutrophils onto inflamed epithelium: a new mechanism to disrupt epithelial intercellular adhesions and promote transepithelial migration. FASEB J. 30, 4007–4020 (2016). www.fasebj.org

KEY WORDS: inflammation · injury · transmigration · intestine · barrier

Epithelial cells lining the intestinal lumen form a selective barrier between the luminal contents and the surrounding tissue. Intestinal epithelial cells (IECs) are held together as continuous polarized sheets by junctional complexes composed of desmosomes and adherens and tight junctions. In addition to mediating cellular adhesion and providing structural support for epithelial monolayers (1), junctional adhesion molecules mediate critical signaling events which maintain epithelial polarity and cell shape (2), and regulate barrier function, cell motility (3–5), proliferation, and differentiation (6, 7). Constituents of the epithelial junctions also play key roles in the regulation of neutrophil [polymorphonuclear leukocyte (PMN)] transepithelial migration (TEM) (8), which is a hallmark of inflammatory mucosal disorders.

PMNs navigating between adjacent epithelial cells encounter a variety of lateral membrane adhesion receptors forming the epithelial junctional complexes. Although some of these receptors can help facilitate PMN TEM, including interactions of signal regulatory protein-α and CD47 (9), others may serve as a barrier for migrating PMNs and are removed from the lateral epithelial surface during TEM. These inlude E-cadherin, a key component of the adherens junctions, and occludin, a component of the tight junctions (10). Desmosomal cadherins are another example of barrier-forming proteins that may be an obstacle for PMNs migrating along the basolateral IEC membrane. Several desmosomal cadherins have been identified in

ABBREVIATIONS: Dsc-2, desmocollin-2; Dsg-2, desmoglein-2; fMLF, formyl-methionyl-leucyl phenylalanine; IBD, inflammatory bowel disease; IEC, intestinal epithelial cell; JAM, junctional adhesion molecule; MMP, matrix metalloproteinase; MP, membrane-derived microparticle; PMN, polymorphonuclear leukocyte; siRNA, small interfering RNA; TEM, transepithelial migration; ZO, zonula occludens

[1] Correspondence: Northwestern University, Tarry Research Building, Room: 3-707, 303 E. Chicago Ave., Chicago, IL 60611, USA. E-mail: ronen.sumagin@northwestern.edu

doi: 10.1096/fj.201600734R
This article includes supplemental data. Please visit *http://www.fasebj.org* to obtain this information.

human epithelium, with desmoglein-2 (DSG-2) being the most abundantly expressed in the intestinal epithelium (11).

Dsg-2 interacts in trans with itself or with desmocollin-2 (Dsc-2) to form transmembrane protein complexes (12). It is linked to the actin cytoskeleton through interactions with adapter proteins, including plakin, plakoglobin, and plakophilin (11). Dsg-2 is a key adhesive component, providing structural support for epithelial monolayers by mediating cell-to-cell adhesions. However, recent evidence suggests that Dsg-2 expression affects the expression and localization of other junctional proteins, thus contributing to the regulation of epithelial barrier function, cell proliferation, motility, and apoptosis (13). As such, loss of Dsg-2 results in decreased expression of Dsc-2 (14), mislocalized expression of junctional proteins zonula occludens (ZO)-1 and coxsackie and adenovirus receptor, resulting in decreased IEC proliferation (15) and impaired barrier (16).

Disruption of mucosal barrier function and epithelial injury are common pathologic features of inflammatory diseases of the gastrointestinal tract. For example, inflammatory bowel diseases encompassing ulcerative colitis and Crohn's disease feature barrier dysfunction and epithelial injury caused by PMN-mediated inflammation (17). Symptoms and severity of inflammation correlate with PMN accumulation in epithelial crypts (18, 19) and decreased expression of key junctional adhesion molecules E-cadherin, ZO-1, and Dsg-2 (20). These data suggest that PMNs migrating across IECs cause tissue damage by altering the expression and localization of junctional adhesion molecules. Indeed, PMN-elastase, which is secreted by activated PMNs during TEM, has been shown to cleave E-cadherin and alter IEC polarity (21). Similarly, PMNs secrete metalloproteinases (MMPs), which are known for the ability to modify extracellular, soluble, and membrane-bound proteins (22). In particular, activated PMNs secrete an abundance of MMP-9 (23, 24), which has been recently shown to cleave Dsg-2, depleting it from cellular junctions (25). Activated PMNs also secrete membrane-derived microparticles (MPs) (26), which are defined as small extracellular vesicles ranging from 0.2 to 1.0 μm in diameter and which contain functional proteins and antigens that are transported across tissues (26). Microparticles have recently come into focus as novel modulators of tissue homeostasis, immunity, and inflammation (27, 28). Proteomic analysis of MPs derived from activated human PMNs has suggested association of MMP-9 with PMN-derived MPs (PMN-MPs) (26).

In the current work we present evidence of enzymatically active MMP-9 that is observed to associate with PMN-MPs. PMN-MPs efficiently bound the epithelial membrane to induce MMP-9-dependent cleavage of Dsg-2. Depletion of Dsg-2 from IEC junctions led to decreased intercellular adhesion, destabilization of IEC monolayers, and enhanced PMN TEM. Given the observation that *en masse* infiltration of mucosal tissues by PMNs is a common feature of pathologic inflammation, accumulation of PMN-MPs containing enzymatically active proteases in the inflamed regions may have significant effects on tissue function and contribute to PMN-associated inflammation and injury of mucosal surfaces.

MATERIALS AND METHODS

Animals

C57BL6J mice (The Jackson Laboratories, Bar Harbor, ME, USA), ages 12–16 wk, were maintained under specific pathogen-free conditions at Northwestern University–Feinberg School of Medicine animal facilities. All experimental protocols were approved by the Institutional Animal Care and Use Committee.

Cells

Human T84 IECs were grown in DMEM-F12 50:50 (Sigma-Aldrich, St. Louis, MO, USA) with supplements (29). PMNs were isolated from human blood obtained from healthy volunteers by density gradient centrifugation (29, 30) and handled according to protocols for the protection of human subjects, as approved by the Northwestern University Institutional Review Board.

Antibodies and reagents

Monoclonal anti-human Dsg-2 (AH12.2) was from Santa Cruz Biotechnology (Santa Cruz, CA, USA); rabbit polyclonal Dsg-2 (EPR6768) and MMP-9 (EP1254) from Abcam (Cambridge, MA, USA); and cell mask orange membrane stain from Molecular Probes (Eugene, OR, USA). Anti-CD11b/CD18 mAb (CBRM1/29) was purified in-house (31), Isotype control IgG1 and anti-Ly6G Abs were from BD Biosciences (San Jose, CA, USA), and HRP-conjugated anti-mouse and anti-rabbit IgGs were from Jackson ImmunoResearch (West Grove, PA, USA). MMP-9 inhibitor II, pan-MMP inhibitor (GM6001), MMP-2 inhibitor IV were from EMD Millipore (Billerica, MA, USA). ABTS (2,2′-azinobis-3-ethylbenzothiazoline-6-sulfonic acid), HBSS with $Ca2^{+}$ and $Mg2^{+}$ ($HBSS^{+}$) and HBSS without Ca^{2+} and Mg^{2+} ($HBSS^{-}$), DMEM including media supplements, Dispase II, chemotactic peptide formyl-methionyl-leucyl phenylalanine (fMLF), and human TNF-α were from Sigma-Aldrich. Murine TNF-α was from PeproTech (Rocky Hill, NJ, USA).

Generation of PMN-MPs

Human PMN-MPs were prepared from the supernatants of fMLF-stimulated PMNs. Freshly isolated PMNs (2×10^7 cells) were stimulated with fMLF (1 μM in 200 μl $HBSS^{+}$, 20 min at 37°C). After stimulation, the supernatants were cleared of cells and cellular debris by 2-stage centrifugation (400 *g* followed by 3000 *g* spins, 10 min) and then subjected to ultracentrifugation at 100,000 *g*. Pelleted MPs were washed and prepared for Western blot analysis, flow cytometry, or functional assays. For all functional assays, MPs derived from 2×10^6 PMNs were used. For preparation of murine PMN-MPs, PMNs were isolated from bone marrow and enriched to ~85–90% purity using Histopaque gradients (1077 and 1119; Sigma-Aldrich) as previously described (32). Murine PMNs (2×10^7 cells) were then stimulated with fMLF (5 μM in 200 μl $HBSS^{+}$, 20 min at 37°C) and MPs were prepared by using centrifugation methods as described above. Enzymatic activity of MMP-9 expressed on MPs derived from both human and mouse PMNs was assessed with a Novex Zymogram gel kit (Thermo Fisher Scientific, Waltham, MA, USA) according to the manufacturer's instructions.

PMN migration assays

In vitro, PMN migration (1×10^6 cell/well in $HBSS^{+}$, 1 h, 37°C) across epithelial monolayers in the physiologically relevant, basolateral-to-apical direction was induced with fMLF gradient

(100 nM) added to low-adhesion plates (33) and quantified by assaying for the PMN myeloperoxidase (29). Postmigration PMNs (after 3 h migration) were collected and immediately used in experiments. *In vivo*, animals were anesthetized by intramuscular injection of ketamine and xylazine mixture at doses of 100 and 5 mg/kg, respectively. A midline abdominal incision was made, and a 4-cm loop of small intestine was exteriorized and clipped at the proximal and distal ends. The loops were injected with MPs (prepared from 5×10^6 bone marrow–derived PMNs), alone or in combination with LPS (100 μg/ml in 200 μl sterile $HBSS^+$) and were reinserted into the peritoneal cavity for 3 h incubation. After incubation, intestinal loops were isolated and lavaged twice with 200 μl $HBSS^+$. The number of $Ly6G^+/CD11b^+$ PMNs in the lavaged fluid (PMNs that migrated into the intestinal lumen) was quantified with flow cytometry. When indicated, pharmacological inhibitors were introduced to intestinal loops in combination with the MP treatment. At the end of all experimental procedures, the animals were euthanized *via* rapid cervical dislocation.

Western blot analysis

IEC monolayers after PMN TEM were lysed in 1% SDS buffer (with 100 mM Tris, pH 7.4) containing protease and phosphatase inhibitors (Sigma-Aldrich) boiled and cleared by centrifugation. Equal amounts of protein (determined with a bicinchoninic acid protein assay) or human and mouse MPs (derived from 2×10^6 PMNs, unless otherwise specified) were separated by SDS-PAGE and transferred onto nitrocellulose membranes. Membranes were blocked (5% nonfat milk in 0.05% Tween-20 Tris-buffered saline) and incubated with appropriate primary antibodies overnight at 4°C, followed by secondary HRP-conjugated antibodies. For protein analysis in cell supernatants, equal protein loading was confirmed by using Ponceau staining. Silencing experiments were performed on subconfluent monolayers (50–70%) grown on permeable supports. Small interfering RNA (siRNA) sequences targeting MMP-9, E-cadherin, and the negative control siRNA were purchased from Santa Cruz Biotechnology. siRNA sequence targeting Dsg-2 was purchased from GE Dharmacon (Lafayette, CO, USA). siRNAs were delivered twice every 12 h in Lipofectamine 3000 at the following concentrations: MMP9 (100 nM), E-cadherin (200 nM), and Dsg-2 (200 nM).

Flow cytometry

PMNs, before or after TEM, were collected and prepared for flow cytometry (33). Total expression of MMP-9 and CD11b was examined after fixation and permeabilization with the Cytofix/Cytoperm kit (BD Biosciences) according to the manufacturer's instructions. Surface protein expression on human and mouse MPs was determined by incubating MPs with fluorescently conjugated antibodies or relevant isotype controls for 40 min on ice. All cell samples were analyzed by FACS Calibur (BD Biosciences) and FlowJo software (Tree Star, Ashland, OR, USA).

Immunofluorescence labeling

IEC monolayers grown on permeable supports before and after PMN TEM or cryosections (7-μm width) of mouse tissue frozen in optimum cutting temperature (OCT) compound (Sakura Finetek, Torrance, CA, USA) were ethanol fixed, blocked with 5% bovine serum albumin in PBS, and incubated with the relevant primary antibody (10 μg/ml, overnight at 4°C), either directly conjugated or followed by an appropriate fluorescently labeled secondary antibody (1 h at room temperature). All images were captured with an LSM 510 confocal microscope (Zeiss, Thornwood, NY, USA) with a plan-Neofluar ×63 oil objective.

TEM

PMN-MPs were resuspended in PBS and fixed by adding an equal volume of 2% paraformaldehyde in 0.1 M phosphate buffer (pH 7.4), to a final volume of 100 μl. Subsequently, PMN-MPs were absorbed onto 400-mesh carbon-coated copper grids (10 min), and imaging was performed with a Tecnai Spirit G2 transmission electron microscope (FEI, Hillsboro, OR, USA).

Mechanical strength (dispase) assay

Confluent IECs in 6-well tissue culture plates were serum starved for 24 h at 37°C, washed with $HBSS^+$ and treated as indicated. Both PMNs and PMN-MPs were incubated with IECs for 6 h. In experiments where pharmacological inhibitors were used, IECs were pretreated with an appropriate inhibitor (37°C in 2 ml serum-free medium) for 1 h before initiation of treatment protocols. After treatments, IECs were washed with $HBSS^+$ and incubated with 2 ml of Dispase solution (5 mg/ml in $HBSS^+$, 30 min at 37°C). Released monolayers were subjected to mechanical stress, and fragments were counted with a dissecting scope (TS100; Nikon, Melville, NY, USA). Data are expressed as the average number of fragments ± SEM.

Statistics

Statistical significance was assessed by Student's *t* test or 1-way ANOVA with a Newman-Keuls multiple-comparison test, by using Prism, ver. 4.0 (GraphPad, La Jolla, CA, USA). Statistical significance was set at $P < 0.05$.

RESULTS

PMN migration across IEC monolayers results in cleavage of E-cadherin and Dsg-2

PMN TEM has been suggested to result in reorganization or loss of adherens and tight junctional complexes, including E-cadherin (20, 34). However, it is still unclear whether expression patterns of desmosomal cadherins, which mediate cellular adhesions, are also affected by transmigrating PMNs. Thus, we investigated the effect of PMN TEM on the expression of Dsg-2, a key component of intestinal epithelial desmosomes (15). PMN TEM assays in the physiologic basolateral to apical direction toward a gradient of fMLF (100 nM, 37°C) were conducted as previously described (33). Three hours after initiation of PMN TEM, IEC lysates and cell supernatants were analyzed for E-cadherin and Dsg-2 expression by Western blot. At this time point, ~90% of total applied PMNs had completed TEM (**Fig. 1*A***).

Consistent with previous observations of PMN-elastase–mediated cleavage of E-cadherin (34), we found decreased expression of E-cadherin in IEC lysates (Fig. 1*B*) and appearance of a 100-kDa fragment in cell supernatants after PMN TEM (Fig 1*B*). PMN TEM also triggered a dramatic loss of Dsg-2. Furthermore, the appearance of a low-molecular-mass band (100 kDa), consistent with the molecular mass for a Dsg-2 cleavage product (25), was observed in IEC lysates, suggesting that the released Dsg-2 fragment binds to IECs in a paracrine fashion. These findings show that transmigrating PMNs

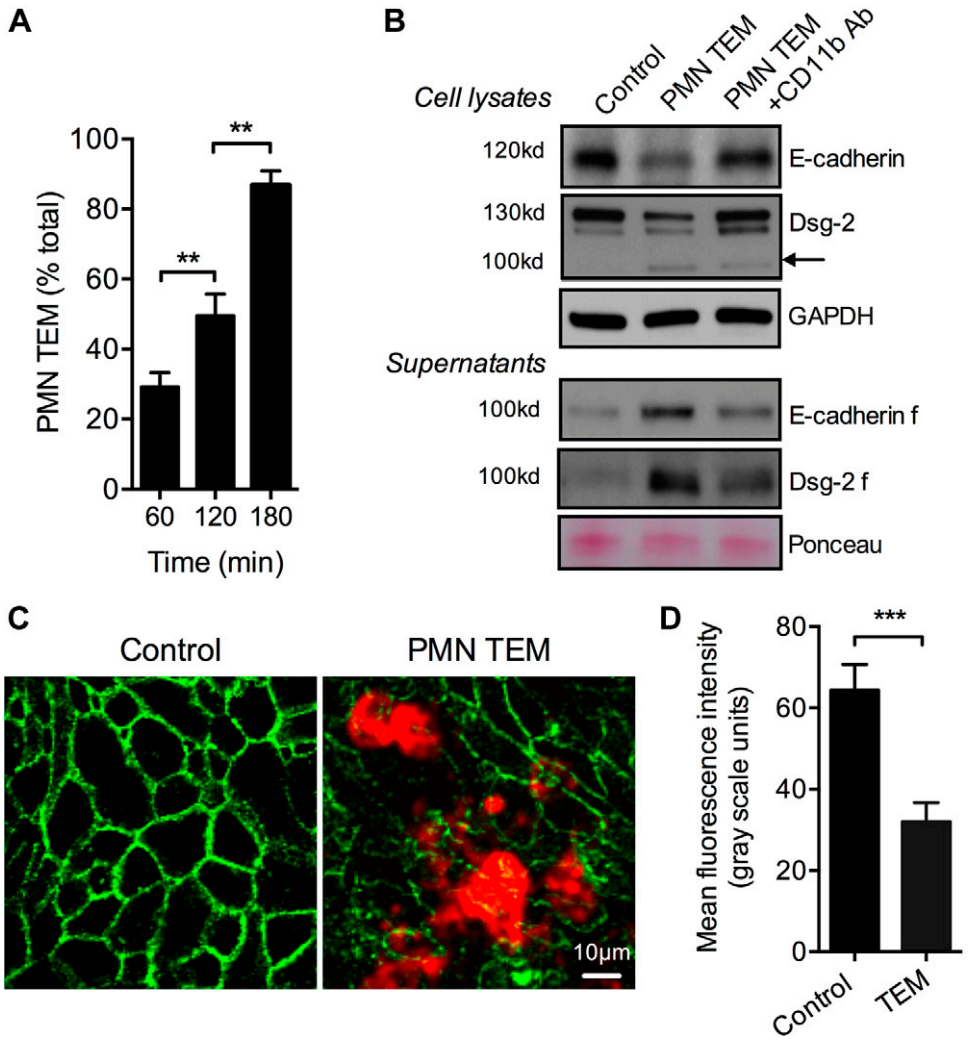

Figure 1. PMN migration across epithelial monolayers results in cleavage of E-cadherin and Dsg-2. PMN migration across IECs in the physiologic basolateral-to-apical direction was induced by the introduction of an fMLF gradient. *A*) At 3 h after initiation of PMN TEM, 87.2 ± 4.1% of the applied PMNs had completed TEM. *B*) Western blot analysis of epithelial cell lysates after PMN TEM (3 h) revealed decreased expression of full-length E-cadherin and Dsg-2. For Dsg-2, appearance of a low-molecular-mass fragment (100 kDa) was observed, consistent with Dsg-2 cleavage product. Cleavage of both cadherins was further confirmed by assaying IEC supernatants after PMN TEM. Equal protein loading in cell supernatants was confirmed with Ponceau protein stain. *C*) Representative immunofluorescence images demonstrate loss of Dsg-2 during PMN TEM compared to control IECs. PMNs were stained for CD11b, red). *D*) The relative fluorescence intensity was quantified in 10 randomly selected fields of view, with and without PMN TEM, as an index of Dsg-2 expression. For immunoblots and fluorescence analysis, data are representative of 3 independent experiments. $^{**}P < 0.01$; $^{***}P < 0.001$.

can induce cleavage of Dsg-2 in a manner similar to that observed for E-cadherin. Indeed analysis of IEC supernatants after PMN TEM revealed the appearance of 100 kDa Dsg-2 fragment confirming Dsg-2 cleavage. Inhibition of PMN TEM using an anti-CD11b function-blocking antibody [10 μg/ml (35)] decreased cleavage of both E-cadherin and Dsg-2. The loss of Dsg-2 during PMN TEM was further confirmed by immunofluorescence confocal microscopy (representative images, Fig. 1*C*, and quantification, Fig. 1*D*).

Transmigrating PMNs secrete MPs with an associated biologically active MMP-9

Circulating and tissue-infiltrating PMNs during inflammation have been shown to modulate cellular function through the secretion of MPs (27, 28, 36). Proteome analysis of human PMN-MPs revealed an abundant expression of MMP-9 (26). Because MMP-9 has been reported to cleave Dsg-2 (25), we hypothesized that PMN-induced cleavage of Dsg-2 during TEM is facilitated by MMP-9 associated with PMN-MPs. As previously described (23), high levels of MMP-9 expression were detected on freshly isolated (unstimulated) permeabilized PMNs (total levels) by flow cytometry (**Fig. 2*A*, *B***). MMP-9 expression was significantly reduced (~50%) after TEM, supporting the idea that PMNs secrete MMP-9 during activation (23). In contrast, expression of membrane-anchored CD11b was not significantly changed. Low-level MMP-9 expression was also observed at the PMN cell surface, but was not significantly altered by TEM (Fig 2*C*, *D*). Consistent with PMN activation, CD11b was mobilized to the cell surface after TEM. Total and cell surface expression of MMP-9 was also evaluated by immunofluorescence staining and confocal microscopy and is shown in representative images (Fig 2*E*). Secretion of MMP-9 was further confirmed by analyzing cell supernatants after PMN TEM (Fig. 2*F*). Abundant levels of MMP-9 were found to be associated with MPs secreted by PMNs during TEM, suggesting that PMN-MPs can be an important source of MMP-9.

Elastase, one of the known PMN-derived proteinases to cleave E-cadherin, was not found to associate with PMN-MPs (not shown). Given this observation, we focused attention on evaluating MMP-9 secretion patterns and its association with PMN-MPs. PMN MMP-9 is primarily contained in gelatinase (tertiary) granules (37) that can be

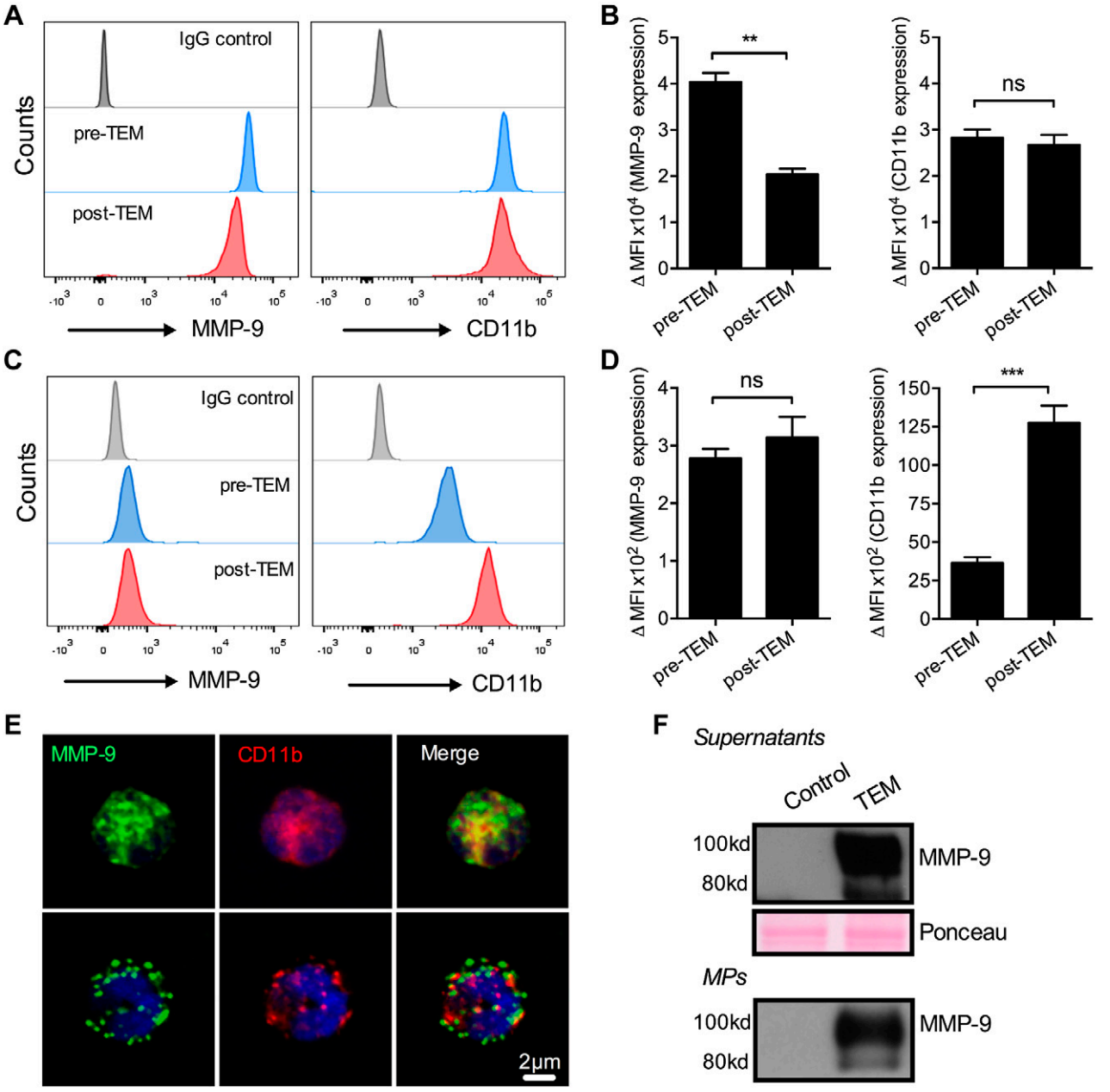

Figure 2. MMP-9 localizes to both PMN granules and cell surface and is secreted during PMN TEM. Expression of MMP-9 on PMNs was examined by using flow cytometric analysis. *A*, *B*) PMNs before and after TEM were fixed, permeabilized, and stained for MMP-9 and CD11b. Representative flow diagrams (*A*) and quantification (*B*) show a significant decrease in total levels of MMP-9 in PMNs after TEM. $^{**}P < 0.01$. *C*, *D*) Analysis of surface expression of PMNs before and after PMN TEM (under nonpermeabilized conditions) revealed detectable basal levels of surface MMP-9. PMN surface expression of MMP-9 was not significantly altered during TEM. ns, not significant. $^{***}P < 0.001$. *E*) Representative immunofluorescence images show total (top) and surface MMP-9 (bottom) expression by permeabilized and nonpermeabilized PMNs, respectively. MMP-9 (green) on PMN surface did not colocalize with CD11b (red). *F*) Release of MMP-9 by transmigrating PMNs was further confirmed by Western blot analysis. Secreted MMP-9 was detected in cell supernatants (soluble form) and associated with PMN-MPs after PMN TEM. Equal protein loading in cell supernatants was confirmed with Ponceau protein stain. For all panels, $n = 3$ independent experiments.

mobilized to release their contents by PMN stimulation with the chemoattractant fMLF (38). Thus, we examined expression of MMP-9 on MPs isolated from fMLF-stimulated PMNs. Using flow cytometry forward and side light scattering, PMN-MPs were compared with 1-μm beads. MPs smaller than 1 μm in diameter that stained positive for phosphatidylserine [annexin V staining of phosphatidylserine has been used to define PMN-derived membrane particles (39)] and CD11b (a PMN marker) were analyzed for MMP-9 expression (**Fig. 3*A***). Heterogeneity in the size of PMN-derived MPs (~100–800 μm) is highlighted by a representative electron microscopic image (Fig. 3*B*). Consistent with reported proteomic analysis data (26), we found high levels of MMP-9 on PMN-MPs by using flow cytometry (Fig. 3*C*) and Western blot analysis (Fig. 3*D*). We next performed zymography analyses to

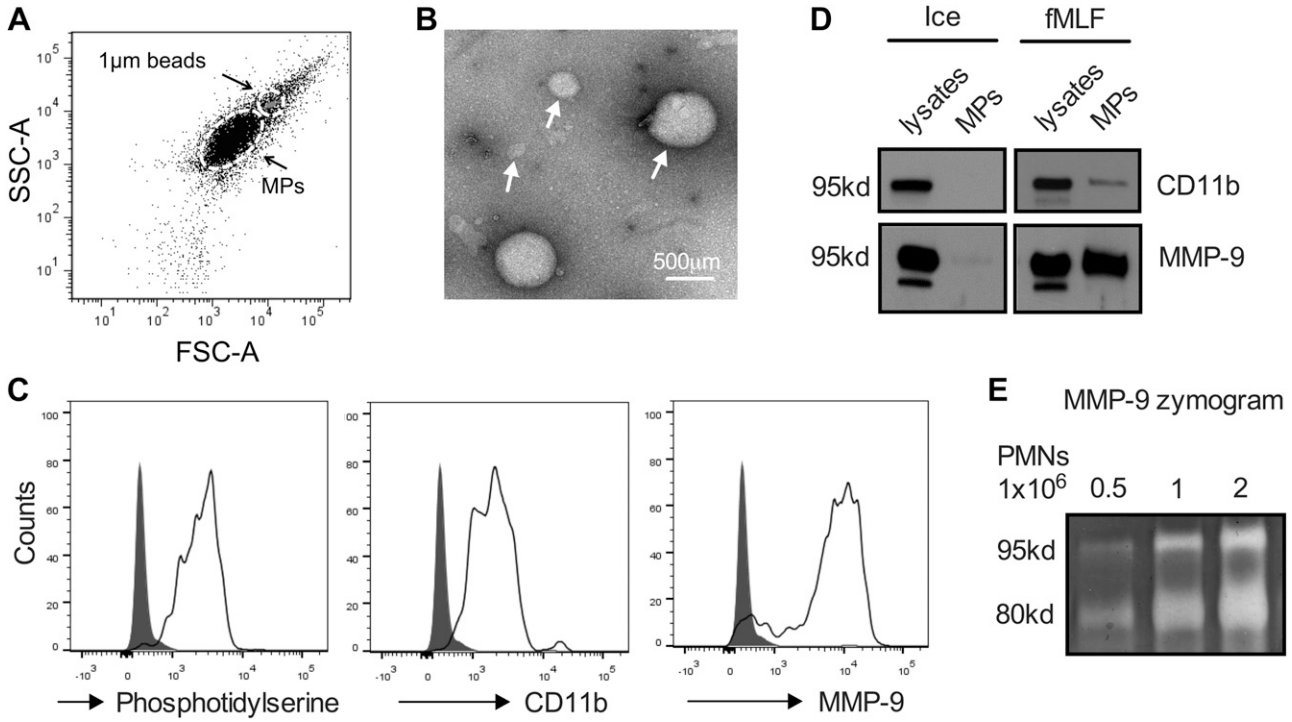

Figure 3. Activated PMNs secrete microparticles with enzymatically active MMP-9. MPs were isolated from supernatants of fMLF-stimulated PMNs (1 μM, 20 min, 37°C). *A*) The presence of PMN-derived MPs (<1 μm) in supernatants of activated PMNs was confirmed by flow cytometry. SSC, side scatter; FSC, forward scatter. *B*) Transmission electron microscopy micrograph depicts the heterogeneity in the size of PMN-derived MPs. *C*) PMN-MPs were further characterized by flow cytometry for the expression of membrane marker, annexin V and the specific myeloid marker CD11b. PMN-MPs that stained positive for both annexin V and CD11b were also found to express high levels of MMP-9. *D*) CD11b and MMP-9 expression on MPs derived from fMLF-stimulated PMNs was also confirmed by Western blot analysis. *E*) Gel zymography confirmed that MP-bound MMP-9 was enzymatically active. MMP-9 enzymatic activity (as evident from collagen degradation) was enhanced with increasing concentration of MPs. All panels are representative of at least 3 independent experiments. Ice, unstimulated PMNs kept on ice at all times.

examine whether MMP-9 associated with PMN-MPs is enzymatically active. Application of PMN-MPs under nonreducing conditions to SDS-PAGE resolving gels containing gelatin as a substrate revealed proteolytic activity of MMP-9 (Fig 3E). MMP-9 activity was enhanced with an increasing number of PMN-MPs. Furthermore, examination of proteolytic activity relative to protein expression (immunoblotting analysis) of MMP-9 on PMN-MPs *vs.* soluble MMP-9 in PMN supernatants that were cleared of MPs (both derived from 1×10^6 PMNs and resuspended in the same volume) revealed ~5-fold higher enzymatic activity of MMP-9 that was associated with PMN-MPs.

Binding of PMN-MPs to IECs leads to MMP-9-dependent cleavage of Dsg-2

After establishing association of enzymatically active MMP-9 with PMN-MPs, we performed concentration curve experiments to examine whether PMN-MPs could bind to IECs and induce cleavage of Dsg-2, as observed during PMN TEM (Fig. 1). In these experiments, MPs isolated from 1, 2, and 3×10^6 PMNs were added to both the basolateral and apical surfaces of IECs that were grown on permeable supports in an inverted orientation (Transwells, Corning, Inc., Corning NY, USA), and IEC cell lysates were analyzed for MMP-9 expression as an index of PMN-MP binding. Increased levels of MMP-9 were observed with increasing amounts of applied MPs (**Fig. 4*A***), suggesting specific contribution of PMN-MPs. We observed the MMP-9 expression by non-cytokine–treated IECs in the absence of MP treatment to be very low and detectable only after high Western blot exposure (shown in **Fig. 6**). PMN-MP binding to IECs (derived from 2×10^6 PMNs, 3 h, 37°C) was further confirmed by immunofluorescence. PMN-MPs that stained positively for CD11b (green) were observed to bind to IEC membrane (red) (Fig. 4*B*). PMN-MP binding to IECs was sufficient to induce cleavage of Dsg-2, but not of the tight junction protein JAM-A or the adherens junction protein E-cadherin (Supplemental Fig. S1*A*). PMN-MP-mediated loss of Dsg-2 was evident in representative immunofluorescence staining and quantification, respectively (Fig 4*C*, *D*). Furthermore, an increase in Dsg-2 cleavage product (100-kDa fragment) was observed in IEC lysates and supernatants after PMN-MP treatment (Fig 4*C*). The loss of Dsg-2 and the increase in Dsg-2 fragment formation (in cell supernatants) was MMP-9 dependent, as it was reversed in the presence of pharmacological inhibitor to MMP-9 (MMP-9 inhibitor II, 100 nM) but not to MMP-2 (MMP-2 inhibitor IV, 200 nM; Fig. 4*D* and Supplemental Fig. S1*B*). Consistent with unstimulated IECs expressing low levels of MMP-9 and in line with previous findings (25),

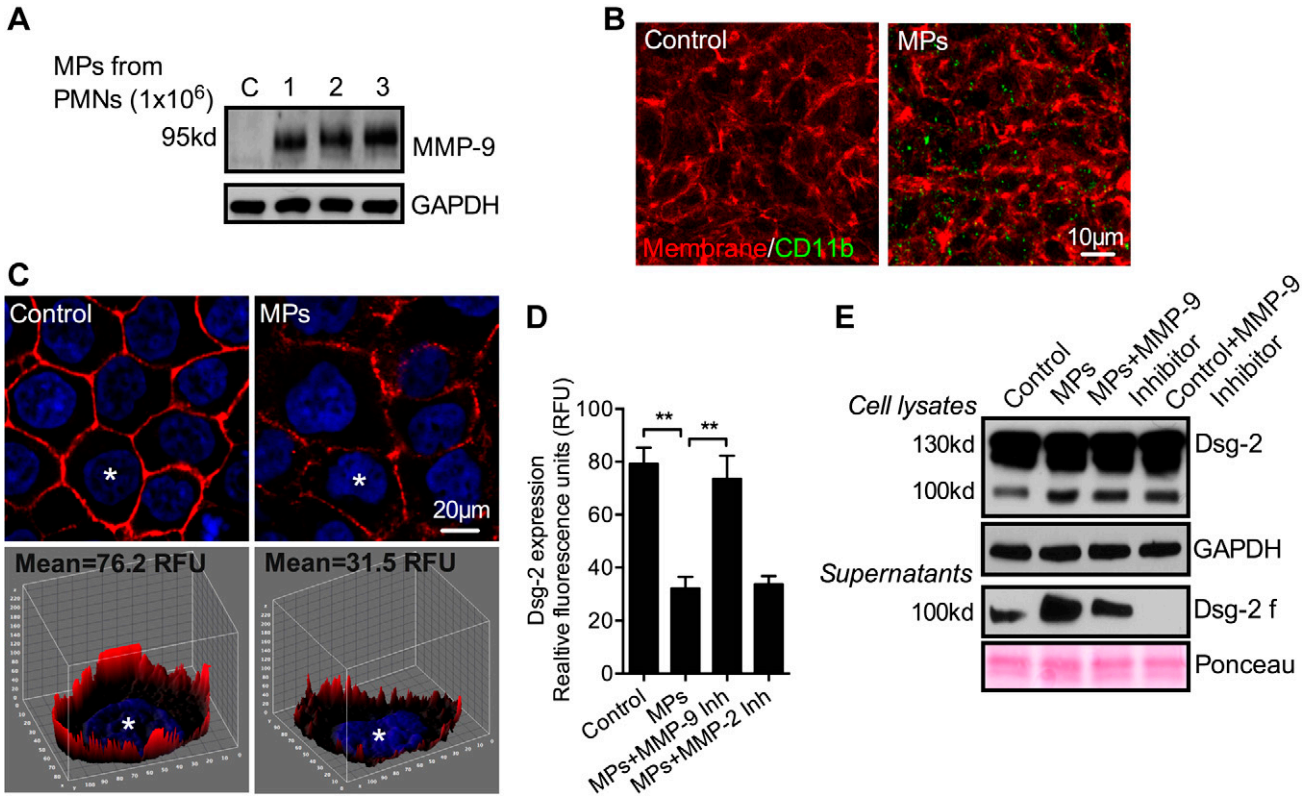

Figure 4. PMN-MP binding to IECs leads to MMP-9-dependent cleavage of Dsg-2. To examine the effect of PMN-MP binding to IEC membrane on Dsg-2 expression and cleavage, PMN-MPs were added to both the upper and lower chambers of cell-migration assay plates, so that both the basolateral and apical IEC surfaces were exposed to treatment (3 h, 37°C). *A*) MPs derived from an increasing number of PMNs (as indicated) were incubated with IECs, and their binding was examined by Western blot analysis. *B*) PMN-MP (derived from 2×10^6 PMNs) binding to IECs was further examined with fluorescence microscopy. Representative immunofluorescence images show that PMN-MPs (positive for CD11b, green) bound to IECs with high efficiency. The IEC surface was visualized with a membrane stain, cell mask (orange). *C*) Representative immunofluorescence images (top) show that PMN-MP binding to epithelial cells led to decreased expression of Dsg-2 (red: Dsg-2; blue: nuclei). A *Z*-stack 3-dimensional surface plot (bottom) shows decreased levels of Dsg-2 expression at the basolateral/apical cell borders. *D*) Quantification of the relative Dsg-2 expression based on fluorescence staining from 3 independent experiments ($n = 50$ cell/condition). $^{**}P < 0.01$. *E*) Western blot analysis confirmed that PMN-MP binding to IECs induced cleavage of Dsg-2. Although constitutive low-level cleavage of Dsg-2 by IECs was observed, treatment with PMN-MPs dramatically increased the abundance of a 100-kDa Dsg-2 cleavage product (Dsg-2 f) both in cell supernatants and in cell lysates. PMN-MP-mediated cleavage of Dsg-2 was MMP-9 dependent, as it was reversed in the presence of an MMP-9 inhibitor (MMP-9 inhibitor II, 100 nM). Constitutive IEC-mediated cleavage of Dsg-2 was similarly suppressed in the presence of MMP-9 inhibitor. Blots are representative of 4 independent experiments.

constitutive low level cleavage of Dsg-2 by IECs was observed under control conditions (no PMN-MPs). Our data suggest that IEC self-cleavage is also dependent on endogenous MMP-9 activity, as it diminished after MMP-9 inhibition (Fig 4*E*). Together, these findings demonstrate that, in addition to endogenous IEC proteinase activity, PMN-MPs may act as a significant source of MMP-9 to cleave Dsg-2.

PMN-MP binding to IECs induces MMP-9 dependent disruption of epithelial cell-to-cell adhesions

Loss of Dsg-2 reduces intercellular adhesion strength, leading to impaired IEC monolayer integrity (40). Given our observation of PMN-MP-mediated cleavage of Dsg-2, we used a well-established Dispase assay (40) to examine whether PMN and PMN-MP binding to IECs could disrupt the integrity of monolayers. PMN adhesion to IECs (2×10^6 cells/well in a 6-well plate, 3 h, 37°C) induced by fMLF (100 nM, had no effect on IECs) triggered a robust fragmentation of epithelial monolayers (**Fig. 5*A***). PMN-MP treatment alone (derived from 2×10^6 PMNs, 3 h, 37°C) was sufficient to achieve similar effects (Fig. 5*B*, *C*). IEC stimulation with TNFα (100 ng) was used as a positive control, as TNFα at this concentration has been shown to activate endogenous, epithelium-derived MMP-9, leading to increased Dsg-2 cleavage and increased monolayer fragmentation (25). Intriguingly, the effect of MPs (derived from 2×10^6 PMNs) was more potent than that of TNFα (100 ng), suggesting that in addition or parallel to endogenous (epithelium-derived) MMP-9, exogenous (PMN-derived) MMP-9 significantly contributes to the regulation of epithelial integrity in conditions of inflammation.

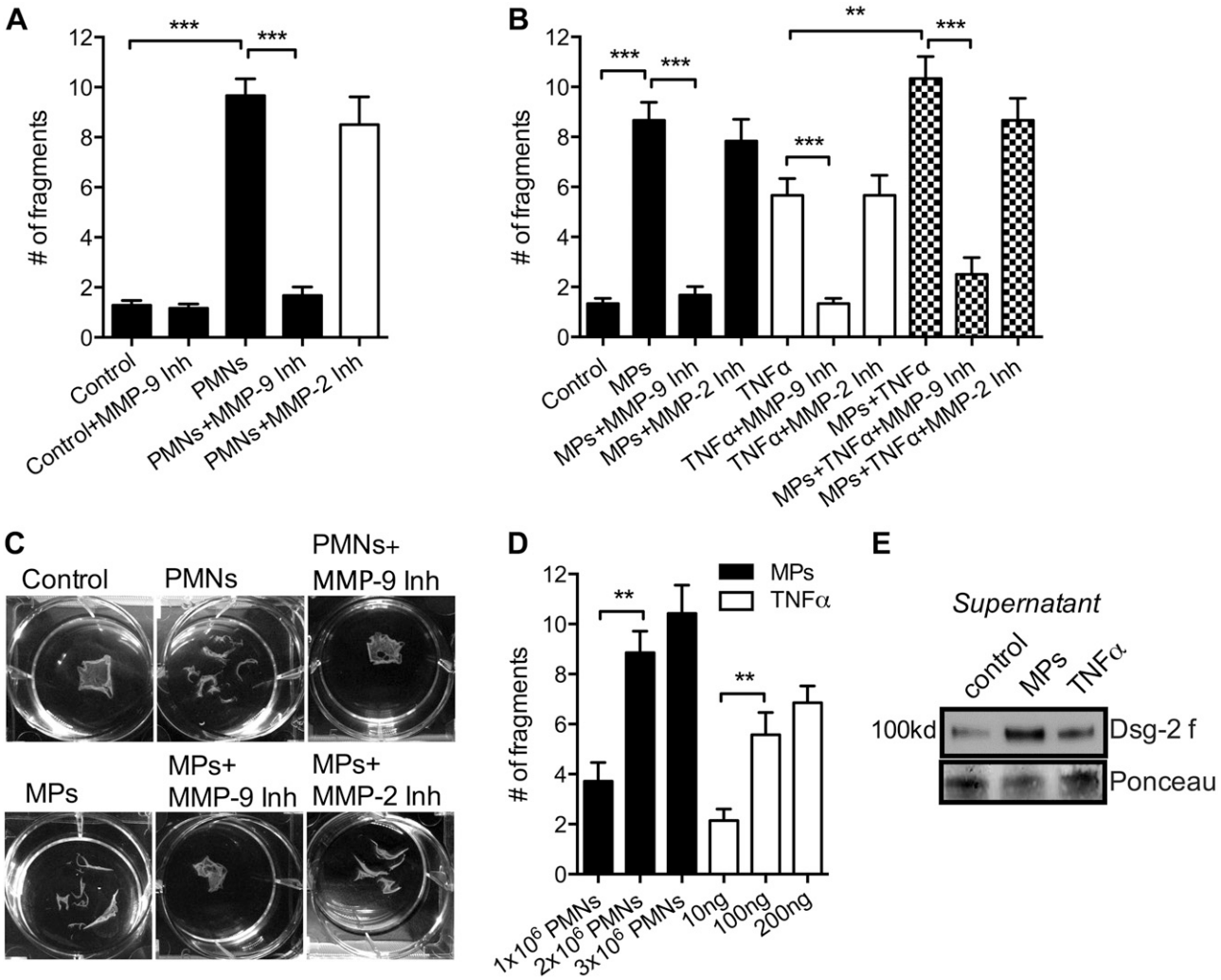

Figure 5. PMN-MP binding to IECs results in MMP-9 dependent disruption of epithelial cell-to-cell adhesions. Dispase-based dissociation assay was used to assess the strength of intercellular adhesions and monolayer integrity after the indicated treatments. *A*) Freshly isolated PMNs were added to IEC monolayers and induced to adhere in the presence of 100 nM fMLF (2×10^6 PMNs/well, 3 h, 37°C). PMN adhesion to IECs resulted in significant fragmentation of IEC monolayers, which was dependent on MMP-9 activity, after Dispase treatment. $^{***}P < 0.001$. Data presented are an average of 3 independent experiments. *B*) Addition of PMN-MPs to IECs (MPs derived from 2×10^6 PMNs, 2 h, 37°C) resulted in significant fragmentation of IEC monolayers, similar to the observed effect of PMNs. TNFα treatment (100 ng) was used as a positive control, as it is known to induce MMP-9 activity in IECs, leading to increased cleavage of Dsg-2. The effects of PMNs and PMN-MPs, as well as TNFα treatment, were dependent on MMP-9 activity and were reversed in the presence of MMP-9 inhibitor (MMP-9 inhibitor II, 100 nM). No cumulative effect of PMN-MP and TNFα treatment was observed. $^{***}P < 0.001$; 3 independent experiments. *C*) Representative images of the Dispase assay showed fragmentation of the IEC monolayers after the specified treatments. *D*) To determine the optimal treatment dose, the effect of an increasing number of PMN-MPs and increasing concentration of TNFα on IEC monolayer fragmentation were examined. *E*) Consistent with the significantly more potent effect of PMN-MPs on monolayer fragmentation compared to TNFα treatment (100 ng), PMN-MP treatment was also more effective in inducing Dsg-2 cleavage.

Dose–response experiments confirmed that increasing the number of PMN-MPs or the concentration of TNFα had no additional effect on the monolayer adhesion strength (Fig. 5*D*).

Consistent with increased monolayer fragmentation induced by PMN-MPs compared with TNFα, under similar conditions PMN-MPs were more effective in mediating Dsg-2 cleavage (Fig. 5*E*). The effects of PMNs, PMN-MPs, and TNFα were reversed in the presence of MMP-9 but not MMP-2 inhibitor, indicating a specific role for MMP-9 in these responses. Together, these findings implicate MP secretion by migrating PMNs and their binding to IECs as a potential mechanism by which PMNs may induce disruption of epithelial intercellular adhesions.

MP deposition by activated PMNs facilitates PMN TEM *in vitro*

Given the ability of PMN-MPs to mediate cleavage of Dsg-2 and disrupt IEC integrity (Figs. 4, 5), we examined the

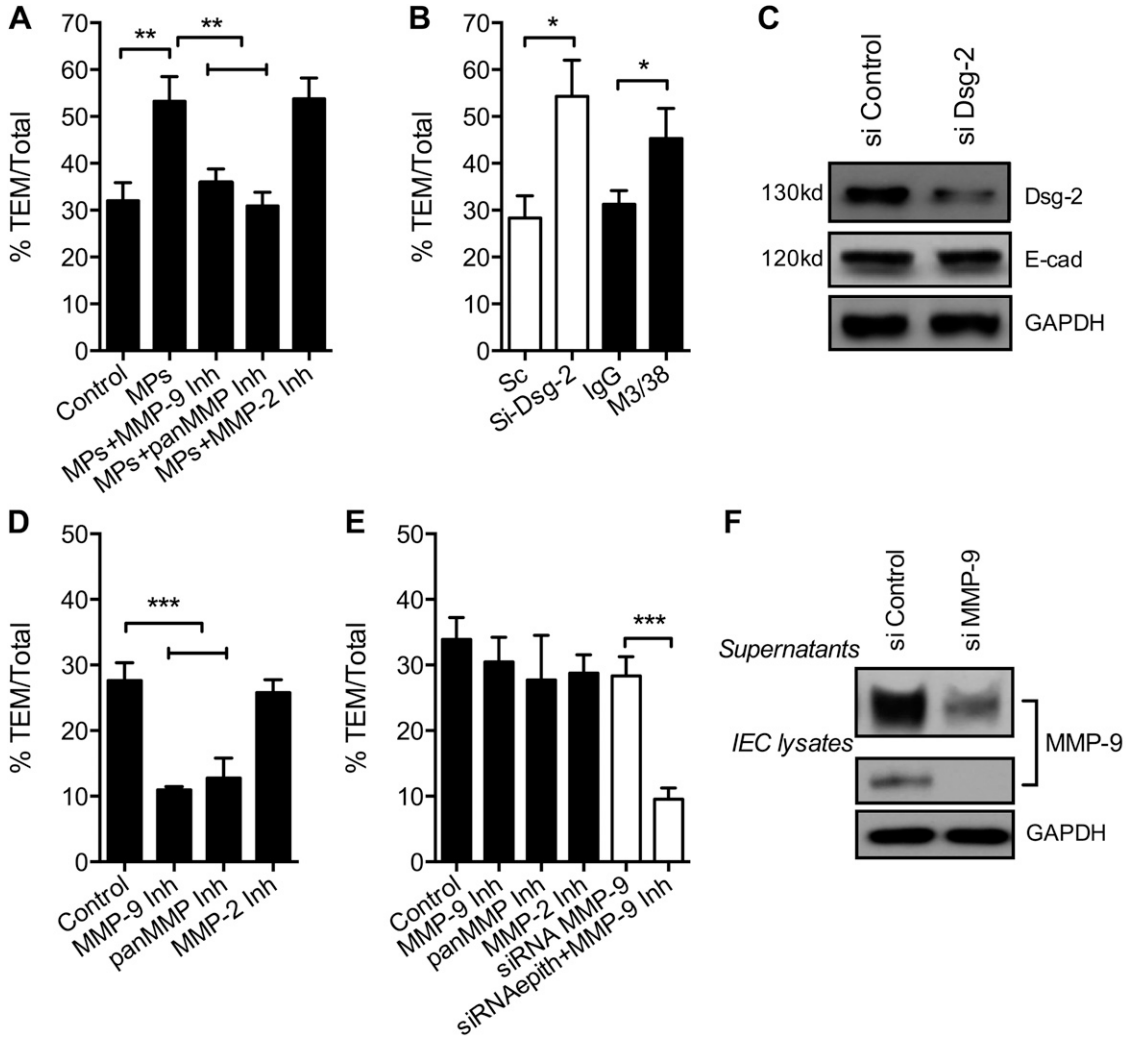

Figure 6. Dsg-2 and PMN-derived MMP-9 collectively regulate PMN TEM. *A*) To examine whether PMN-MP binding to IECs can affect PMN TEM, assays were performed after IEC preincubation with PMN-MPs (derived from 2×10^6 PMNs, 3 h, 37°C). MP treatment of IECs significantly enhanced PMN TEM. The increase in PMN TEM was prevented by the addition of MMP-9, but not by MMP-2 inhibitors. $^{**}P < 0.01$. *B*) To determine the contribution of Dsg-2 to the regulation of PMN TEM, PMN TEM assays were performed after siRNA- or antibody (anti-Gal-3 inhibitory antibody, M3/38)-mediated down-regulation of Dsg-2. Loss of Dsg-2 resulted in significantly enhanced PMN TEM, similar to that observed with PMN-MPs. $^{*}P < 0.05$. *C*) The efficiency of Dsg-2 down-regulation by siRNA is shown by representative immunoblots. *D*) To establish the role of IEC-derived MMP-9 in PMN TEM, IEC monolayers were pretreated with pharmacological MMP inhibitors (MMP-9 inhibitor II, 100 nM; pan-MMP inhibitor, GM6001, 10 μM; or MMP-2 inhibitor IV, 200 nM, 1 h, 37°C) or with MMP-9 siRNA. Immediately before the addition of PMNs, IECs were washed, so that migrating PMNs were not exposed to the inhibitors. No significant effects of inhibitors on PMN TEM were observed. $^{***}P < 0.001$. *E*) PMN TEM assays were performed in the presence of MMP inhibitors (added to the top chamber of cell-migration assay plates at the same time as PMNs) to ensure exposure of both PMNs and IECs. Inhibition of MMP-9 using specific MMP-9 inhibitor or pan-MMP inhibitor, but not MMP-2 inhibitor, significantly decreased PMN TEM. $^{***}P < 0.001$. *F*) The efficiency of MMP-9 down-regulation by siRNA both in cell lysates and in supernatants (secreted MMP-9) is shown by representative immunoblots. *A*, *B*, *D*, *E*) Three independent experiments where at least 3 migration assays were used for each condition. *C*, *F*) Immunoblots are representative of 3 independent experiments.

possibility that MP deposition onto IECs by PMNs serves as a mechanism to promote PMN TEM. In these experiments, PMN TEM assays (33, 35) were performed after pretreatment of T84 IECs with PMN-MPs (derived from 2×10^6 PMNs, 3 h, 37°C). Consistent with the observed PMN-MP-induced loss of Dsg-2 and disruption of cell-to-cell adhesions, pretreatment of IECs with PMN-MPs elicited a significant increase in PMN TEM (Fig. 6*A*). The PMN-MP-mediated increase in PMN TEM was reversed with the addition of general MMP and specific MMP-9 inhibitors (GM6001, 100 μM, and MMP-9 inhibitor II, 100 nM, respectively) but not an inhibitor of MMP-2 (MMP-2 inhibitor IV, 200 nM). We further established that PMN-MPs did not directly induce PMN-chemotaxis (not shown), confirming the role for PMN-MP associated MMP-9 in regulation of PMN TEM.

To determine whether Dsg-2 contributes to the regulation of PMN TEM and confirm that the observed PMN-MP effects were due to loss of Dsg-2, PMN TEM was examined after siRNA–mediated down-regulation of Dsg-2 or after IEC treatment with an inhibitory anti-galectin (Gal)-3 antibody (M3/38). We recently established that

M3/38 inhibits Gal-3 binding to Dsg-2, leading to its depletion from epithelial junctions (40). For both treatments, down-regulation of Dsg-2 resulted in significant increases in PMN TEM (Fig. 6*B*), similar to the observed effects of PMN-MPs. The efficiency of Dsg-2 down-regulation by siRNA is shown by representative immunoblots (Fig. 6*C*). The down-regulation had no effect on levels of E-cadherin. These findings suggest that Dsg-2 serves as a barrier for transmigrating PMNs and that PMN-MPs, by removing Dsg-2 from junctions, promote PMN TEM.

PMN-derived MMP-9 facilitates PMN TEM

Depending on the cell type used, MMP-9 has been found to either promote (41) or not to be involved (42) in PMN transmigration. The findings in this study suggest that, in IECs, MMP-9 facilitates PMN TEM by mediating Dsg-2 cleavage. To directly test this idea, we conducted PMN TEM assays in the presence of pan-MMP, specific MMP-9, and control MMP-2 inhibitors. Treatment with both pan-MMP and MMP-9, but not MMP-2 inhibitors, significantly attenuated PMN TEM (Fig. 6*D*), confirming the role of MMP-9 in facilitating this process. Similar increases in PMN TEM were obtained with preincubation of PMNs with inhibitors before the initiation of PMN TEM (data not shown), suggesting an important contribution of PMN-derived MMP-9 to PMN TEM.

Because IECs express endogenous MMP-9, we also examined the potential contribution of IEC-derived MMP-9 to PMN TEM. In these experiments IECs were pretreated with the aforementioned inhibitors (40 min, 37°C), which were then removed and PMN TEM assays were performed. Neither inhibitor had a significant effect on PMN TEM (Fig. 6*E*). Similar results were obtained when PMN TEM assays were conducted after siRNA-mediated down-regulation of IEC MMP-9 expression (Fig. 6*E*). Under siRNA conditions, the addition of an MMP-9 inhibitor to migrating PMNs significantly attenuated PMN TEM. The decrease in MMP-9 expression after siRNA treatment was confirmed both in IEC lysates and IEC supernatants by immunoblot analysis (Fig. 6*F*). Together, these findings suggest that PMN-derived MMP-9 rather then IEC MMP-9 plays an important role in PMN TEM.

PMN-MPs promote cleavage of Dsg-2 *in vivo* to increase PMN TEM

To examine the effect of PMN-MPs on Dsg-2 expression and PMN recruitment *in vivo*, we isolated murine MPs from fMLF (5 μM)-stimulated bone marrow–derived PMNs (mPMN-MPs; confirmed to display active MMP-9; Fig. 7*A*) and introduced them into ligated murine ileal loops (MPs derived from 5×10^6 PMNs, 3 h). The number of PMNs that migrated into the intestinal lumen and the mucosal tissue was quantified by flow cytometry of lavaged ileal loops (200 μl sterile $HBSS^+$) and immunofluorescence labeling (35).

Consistent with observations in cultured IECs, mPMN-MP treatment triggered dramatic loss of Dsg-2 from the apical epithelial junctional complexes (representative immunofluorescence images, Fig. 7*B*). Paralleling loss of Dsg-2, a significant influx of PMNs into the intestinal lumen and the mucosal tissue was observed after treatment with mPMN-MP (representative flow diagrams, Fig. 7*C*, and fluorescence images, Fig. 7*E*). As expected, no PMNs were detected in the lumen of control intestines.

Addition of lipopolysaccharide (LPS, 100 μg/ml, 1 h) in combination with mPMN-MPs treatment (LPS was added 2 h after initial administration of PMN-MP) further increased the number of PMNs infiltrating the intestinal lumen. Administration of LPS alone into ligated ileal loops induced only moderate PMN migration (Fig. 7*D*), without having significant effects on Dsg-2 expression (not shown). Similar to *in vitro* observations, mPMN-MP induced loss of Dsg-2 and increased PMN TEM *in vivo*, were MMP-9 dependent, and were diminished in the presence of MMP-9 (5 mg/kg body weight) and pan-MMP (100 mg/kg body weight, not shown), but not MMP-2 (10 mg/kg body weight) inhibitors. Finally, to examine whether Dsg-2 is involved in the regulation of PMN TEM *in vivo*, we used an established approach (35, 42), where administration of M3/38 (an anti-Gal3 mAb, 50 μg, 2 h) into ligated ileal loops resulted in acute depletion of Dsg-2 in intestinal epithelium (40). M3/38 but not IgG control antibody triggered increased PMN infiltration of the intestinal lumens (Fig. 7*D*). M3/38-mediated loss of Dsg-2 is a result of increased Dsg-2 internalization and proteasome degradation but not cleavage (40). Thus, as expected, the observed M3/38-induced increases in PMN TEM were MMP-9 independent. Together, these findings suggest that PMN-MPs released during PMN TEM cleave Dsg-2 *via* an MMP-9-dependent mechanism and impair IEC integrity and facilitate increases in PMN recruitment *in vivo*.

DISCUSSION

PMN migration across epithelial monolayers under the conditions of inflammation often leads to barrier dysfunction and tissue injury (17, 33). Release of MPs by various cell types, including activated PMNs, has recently come into focus as a new mechanism of cellular communication. Indeed, MPs generated by platelets and endothelial cells have been implicated in several vascular diseases, where they were shown to contribute to regulation of the coagulation cascade and vascular homeostasis (36). Although the function of PMN-MPs is less understood, there is evidence that PMN-MPs become highly enriched at sites of inflammation (28, 43). PMN-MPs were further suggested to be biologically active and respond to external stimuli by generating ROS or producing leukotriene B_4 (26). In the current work, we demonstrate that activated PMNs during TEM secrete MPs that display high levels of enzymatically active MMP-9. It is not yet clear whether the MMP-9 that is carried by PMN-MPs is packaged inside or is

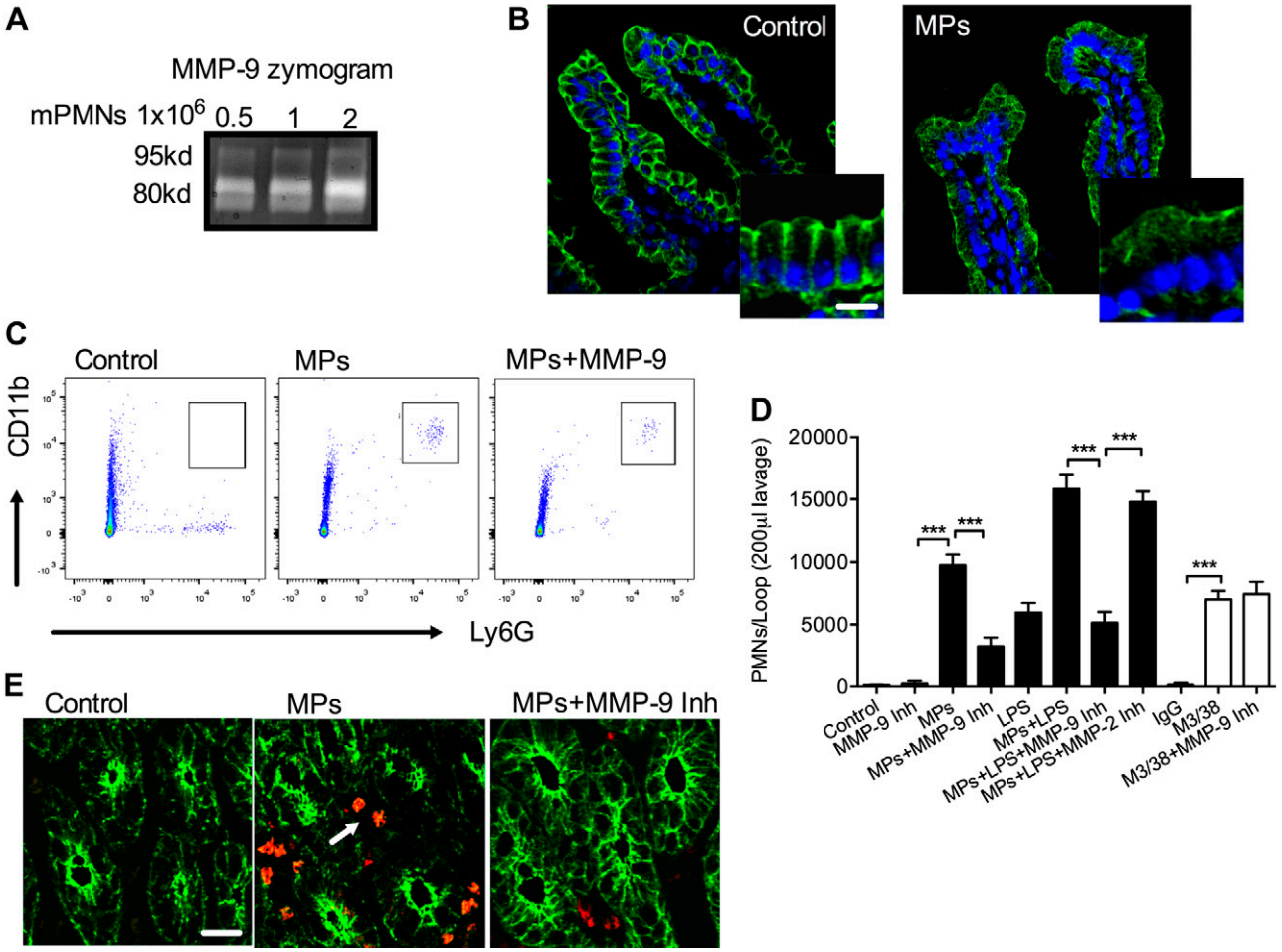

Figure 7. PMN-MP treatment of murine intestines promotes PMN TEM *in vivo*. Murine MPs were prepared from bone marrow–derived PMNs. *A*) Gel zymography was used to confirm that mPMN-MPs expressed enzymatically active MMP-9. MMP-9 enzymatic activity (as evident from collagen degradation) was enhanced with an increasing concentration of MPs. *B*) To examine the effect of mPMN-MPs on Dsg-2 expression and distribution *in vivo*, mPMN-MPs were administered intraluminally into ligated ileal loops (MPs were derived from 5×10^6 PMNs for 3 h). After PMN-MP incubation, tissue from ileal loops was prepared for immunofluorescence imaging analysis. A dramatic loss of Dsg-2 (green) from the apical junctional regions was observed. Scale bar, 50 μm. *C–E*) In separate experiments, after mPMN-MP treatment, PMNs that migrated into the lumen were isolated by lavage and quantified using flow cytometric analysis. *C*) Representative flow diagrams ($n = 5$ mice/condition) depict mPMN-MP-induced PMN migration into the intestinal luminal space. PMN migration was further potentiated with the addition of LPS or M3/38-mediated down-regulation of Dsg-2. *D*) Quantification of data from *C*. *E*) Representative immunofluorescence images of cryosections from the ileum show PMN infiltration (red) of the intestinal epithelia (outlined by actin staining, green) and the lumen after mPMN-MP treatment ($n = 5$ mice/condition). Scale bar, 50 μm.

associated with the MP surface; however, PMN-MP binding to IECs induced MMP-9-dependent cleavage of Dsg-2, leading to impaired IEC integrity. Although other proteolytic cleavage events are likely to occur during PMN TEM, our findings demonstrate PMN-MP-mediated cleavage of Dsg-2, but not E-cadherin or JAM-A, supporting a role for Dsg-2 in TEM.

MMP-9 localizes primarily to PMN granules (31, 44); however, we observed low MMP-9 expression on the PMN surface. Although it is possible that low MMP-9 expression on PMN surface is a result of mild PMN activation during the isolation process, the observation that MMP-9 surface expression did not change after activation, and TEM suggests otherwise.

Immunofluorescence staining revealed that MMP-9 exhibited punctate distribution similar to that reported for CD11b (45), but did not colocalize with CD11b, which is typically expressed on membrane ruffles (46). It remains to be determined whether MMP-9 expressed at the PMN surface associates with another protein or nonspecifically coats PMN membranes. The total levels of PMN MMP-9 were significantly decreased after PMN TEM. Decreased levels of MMP-9 were accompanied by an increased presence of MMP-9 in cell supernatants, consistent with the previously established release of MMP-9 by activated PMNs.

Consistent with recent proteomic analysis that revealed the presence of MMP-9 on MPs derived from fMLF-activated PMNs (26), we found abundant association of MMP-9 with PMN-MPs. We further established that MMP-9 carried by PMN-MPs exhibited high proteolytic activity (assessed by collagen degradation) and thus could mediate changes in the surrounding tissue. Moreover, PMN-MP-bound MMP-9 exhibited

higher activity compared to MMP-9 secreted in the soluble form. Soluble MMP-9 could add to the effects of PMN-MP-bound MMP-9; however, its relative contribution compared to PMN-MP-bound MMP-9 remains to be determined. MPs have been suggested to increase stability and improve transport of functional proteins across tissue (47). Thus, tissue-infiltrating PMNs releasing MPs carrying MMP-9 with high proteolytic activity may be a mechanism to ensure efficient remodeling of the epithelial monolayers and the surrounding matrix during TEM. Indeed, tissue remodeling is essential for proper PMN trafficking. As such, inability to remodel endothelial junctional components, such as VE-cadherin (48), cell cytoskeleton (49), and the extracellular matrix (50), inhibits PMN transmigration.

PMN-MPs are emerging as important contributors to regulation of tissue function and homeostasis; however, whether they mediate beneficial or adverse effects under inflammatory conditions is still unclear. For example, PMN-MP binding to endothelial cells has been suggested to be proinflammatory and induce cell injury (51), whereas MPs binding to PMNs decrease the PMNs' ability to adhere and migrate across endothelial cells (39). Similarly, binding of PMN-MPs to natural killer cells and macrophages exerts an anti-inflammatory activity diminishing their responses, thus potentially favoring the resolution of inflammation (28, 52). Finally, the ability of PMN-derived microvesicles to enter cartilage has been recently shown to protect the joint in inflammatory arthritis (43).

In our setup, binding of PMN-MPs to polarized IECs induced MMP-9-dependent cleavage of Dsg-2, leading to impaired integrity of IEC monolayers and increased PMN tissue infiltration. Indeed, in inflammatory bowel diseases, which are characterized by a high number of infiltrating PMNs, decreased Dsg-2 expression correlates with increased inflammation and severity of the disease (19). Furthermore, cleaved ectodomains of Dsg-2 have been detected in inflamed intestinal mucosa of colitic mice and patients with ulcerative colitis (25). As has been recently demonstrated by Kamekura *et al.* (25), and confirmed in this work, secretion of proinflammatory cytokines, such as TNFα or IFNγ, by IECs or tissue infiltrating leukocytes can trigger activation of IEC MMPs, leading to Dsg-2 cleavage and epithelial dysfunction. Our current findings suggest that, during acute inflammation that is characterized by a high number of mucosa-infiltrating PMNs, PMN-MPs may serve as another major source of MMP-9 and exert inflammatory effects, contributing to tissue injury and symptomatic disease.

Our findings further suggest that Dsg-2 serves as a barrier for transmigrating PMNs, preventing both PMN tissue accumulation and the resulting tissue damage. Thus, stabilizing Dsg-2 at the cell junctions or developing methodologies to prevent its cleavage may prove to be effective approaches to promoting the resolution of inflammation. Similarly, our study suggests a role for MMP-9 in regulating PMN migration across IECs, because of its ability to cleave Dsg-2 and remove its inhibitory effects on PMN TEM. Supporting this idea, PMN migration across endothelial cells, which in most cases do not express Dsg-2, has been found to be MMP-9 independent (53).

Finally, loss of Dsg-2 and E-cadherin is considered a hallmark of epithelial-to-mesenchymal transition, given that they serve to maintain epithelial cell polarity and prevent cell migration and invasion of other tissues (54, 55). The observation that PMNs can deposit MPs rich in MMP-9 onto epithelial surfaces, where MMP-9 can mediate cleavage of Dsg-2, may implicate tissue-infiltrating PMNs in promoting tumorigenesis. These data thus provide a direct link between inflammation and cancer, strengthening the prevailing view that immune cell–mediated inflammation is a major risk factor for the development of various malignancies, including lung, ovarian, colorectal, and pancreatic carcinomas (56, 57).

In summary, the current work demonstrated that tissue-infiltrating PMNs release MPs with enzymatically active MMP-9 that binds to IECs and triggers acute remodeling of epithelial junctions and decreased inter-epithelial adhesions, leading to enhanced recruitment of PMNs. Our studies define a new mechanism by which PMNs infiltrating the intestinal mucosa disrupt IEC junctions to facilitate PMN TEM, thus likely contributing to disease pathology in a variety of inflammatory conditions. FJ

ACKNOWLEDGMENTS

The authors thank Dr. J. Koch (Northwestern University) and the Northwestern University Center for Advanced Microscopy Core Facility [supported by U.S. National Institutes of Health (NIH), National Cancer Institute Grant CCSG P30 CA060553 awarded to the Robert H. Lurie, Comprehensive Cancer Center] for help with electron microscopic imaging of the PMN-MPs. The authors also thank Lorrain Mascarenhas (Northwestern University) for technical assistance and proofreading of the manuscript. This work was supported by NIH, National Institute of Diabetes and Digestive and Kidney Diseases Grants DK072564, DK061379, and DK079392 (to C.A.P.); DK055679 and DK059888 (to A.N.); and DK101675, as well as American Cancer Society IRG-9303718 (to R.S.). The authors declare no conflicts of interest.

AUTHOR CONTRIBUTIONS

V. Butin-Israeli and R. Sumagin designed and performed the research, analyzed the data, and wrote the paper; M. C. Houser and M. Feng performed the research and analyzed the data; and E. B. Thorp, A. Nusrat, and C. A. Parkos designed the research and wrote the paper.

REFERENCES

1. Farquhar, M. G., and Palade, G. E. (1963) Junctional complexes in various epithelia. *J. Cell Biol.* **17**, 375–412
2. Shin, K., Fogg, V. C., and Margolis, B. (2006) Tight junctions and cell polarity. *Annu. Rev. Cell Dev. Biol.* **22**, 207–235
3. Matsuda, M., Kubo, A., Furuse, M., and Tsukita, S. (2004) A peculiar internalization of claudins, tight junction-specific adhesion

molecules, during the intercellular movement of epithelial cells. *J. Cell Sci.* **117**, 1247–1257
4. Du, D., Xu, F., Yu, L., Zhang, C., Lu, X., Yuan, H., Huang, Q., Zhang, F., Bao, H., Jia, L., Wu, X., Zhu, X., Zhang, X., Zhang, Z., and Chen, Z. (2010) The tight junction protein, occludin, regulates the directional migration of epithelial cells. *Dev. Cell* **18**, 52–63
5. Severson, E. A., Jiang, L., Ivanov, A. I., Mandell, K. J., Nusrat, A., and Parkos, C. A. (2008) Cis-dimerization mediates function of junctional adhesion molecule A. *Mol. Biol. Cell* **19**, 1862–1872
6. Nava, P., Capaldo, C. T., Koch, S., Kolegraff, K., Rankin, C. R., Farkas, A. E., Feasel, M. E., Li, L., Addis, C., Parkos, C. A., and Nusrat, A. (2011) JAM-A regulates epithelial proliferation through Akt/β-catenin signalling. *EMBO Rep.* **12**, 314–320
7. Zihni, C., Balda, M. S., and Matter, K. (2014) Signalling at tight junctions during epithelial differentiation and microbial pathogenesis. *J. Cell Sci.* **127**, 3401–3413
8. Sumagin, R., and Parkos, C. A. (2015) Epithelial adhesion molecules and the regulation of intestinal homeostasis during neutrophil transepithelial migration. *Tissue Barriers* **3**, e969100
9. Liu, Y., Bühring, H. J., Zen, K., Burst, S. L., Schnell, F. J., Williams, I. R., and Parkos, C. A. (2002) Signal regulatory protein (SIRPalpha), a cellular ligand for CD47, regulates neutrophil transmigration. *J. Biol. Chem.* **277**, 10028–10036
10. Chun, J., and Prince, A. (2009) TLR2-induced calpain cleavage of epithelial junctional proteins facilitates leukocyte transmigration. *Cell Host Microbe* **5**, 47–58
11. Bornslaeger, E. A., Corcoran, C. M., Stappenbeck, T. S., and Green, K. J. (1996) Breaking the connection: displacement of the desmosomal plaque protein desmoplakin from cell-cell interfaces disrupts anchorage of intermediate filament bundles and alters intercellular junction assembly. *J. Cell Biol.* **134**, 985–1001
12. Garrod, D., and Chidgey, M. (2008) Desmosome structure, composition and function. *Biochim. Biophys. Acta* **1778**, 572–587
13. Nava, P., Laukoetter, M. G., Hopkins, A. M., Laur, O., Gerner-Smidt, K., Green, K. J., Parkos, C. A., and Nusrat, A. (2007) Desmoglein-2: a novel regulator of apoptosis in the intestinal epithelium. *Mol. Biol. Cell* **18**, 4565–4578
14. Kolegraff, K., Nava, P., Helms, M. N., Parkos, C. A., and Nusrat, A. (2011) Loss of desmocollin-2 confers a tumorigenic phenotype to colonic epithelial cells through activation of Akt/β-catenin signaling. *Mol. Biol. Cell* **22**, 1121–1134
15. Kamekura, R., Kolegraff, K. N., Nava, P., Hilgarth, R. S., Feng, M., Parkos, C. A., and Nusrat, A. (2014) Loss of the desmosomal cadherin desmoglein-2 suppresses colon cancer cell proliferation through EGFR signaling. *Oncogene* **33**, 4531–4536
16. Lie, P. P., Cheng, C. Y., and Mruk, D. D. (2010) Crosstalk between desmoglein-2/desmocollin-2/Src kinase and coxsackie and adenovirus receptor/ZO-1 protein complexes, regulates blood-testis barrier dynamics. *Int. J. Biochem. Cell Biol.* **42**, 975–986
17. Brazil, J. C., Louis, N. A., and Parkos, C. A. (2013) The role of polymorphonuclear leukocyte trafficking in the perpetuation of inflammation during inflammatory bowel disease. *Inflamm. Bowel Dis.* **19**, 1556–1565
18. Xavier, R. J., and Podolsky, D. K. (2007) Unravelling the pathogenesis of inflammatory bowel disease. *Nature* **448**, 427–434
19. Langhorst, J., Elsenbruch, S., Mueller, T., Rueffer, A., Spahn, G., Michalsen, A., and Dobos, G. J. (2005) Comparison of 4 neutrophil-derived proteins in feces as indicators of disease activity in ulcerative colitis. *Inflamm. Bowel Dis.* **11**, 1085–1091
20. Kucharzik, T., Walsh, S. V., Chen, J., Parkos, C. A., and Nusrat, A. (2001) Neutrophil transmigration in inflammatory bowel disease is associated with differential expression of epithelial intercellular junction proteins. *Am. J. Pathol.* **159**, 2001–2009
21. Ginzberg, H. H., Cherapanov, V., Dong, Q., Cantin, A., McCulloch, C. A., Shannon, P. T., and Downey, G. P. (2001) Neutrophil-mediated epithelial injury during transmigration: role of elastase. *Am. J. Physiol. Gastrointest. Liver Physiol.* **281**, G705–G717
22. Stamenkovic, I. (2003) Extracellular matrix remodelling: the role of matrix metalloproteinases. *J. Pathol.* **200**, 448–464
23. Ardi, V. C., Kupriyanova, T. A., Deryugina, E. I., and Quigley, J. P. (2007) Human neutrophils uniquely release TIMP-free MMP-9 to provide a potent catalytic stimulator of angiogenesis. *Proc. Natl. Acad. Sci. USA* **104**, 20262–20267
24. Lindsey, M., Wedin, K., Brown, M. D., Keller, C., Evans, A. J., Smolen, J., Burns, A. R., Rossen, R. D., Michael, L., and Entman, M. (2001) Matrix-dependent mechanism of neutrophil-mediated release and activation of matrix metalloproteinase 9 in myocardial ischemia/reperfusion. *Circulation* **103**, 2181–2187
25. Kamekura, R., Nava, P., Feng, M., Quiros, M., Nishio, H., Weber, D. A., Parkos, C. A., and Nusrat, A. (2015) Inflammation-induced desmoglein-2 ectodomain shedding compromises the mucosal barrier. *Mol. Biol. Cell* **26**, 3165–3177
26. Dalli, J., Montero-Melendez, T., Norling, L. V., Yin, X., Hinds, C., Haskard, D., Mayr, M., and Perretti, M. (2013) Heterogeneity in neutrophil microparticles reveals distinct proteome and functional properties. *Mol. Cell. Proteomics* **12**, 2205–2219
27. Johnson, B. L. III, Kuethe, J. W., and Caldwell, C. C. (2014) Neutrophil derived microvesicles: emerging role of a key mediator to the immune response. *Endocr. Metab. Immune Disord. Drug Targets* **14**, 210–217
28. Pliyev, B. K., Kalintseva, M. V., Abdulaeva, S. V., Yarygin, K. N., and Savchenko, V. G. (2014) Neutrophil microparticles modulate cytokine production by natural killer cells. *Cytokine* **65**, 126–129
29. Parkos, C. A., Colgan, S. P., Delp, C., Arnaout, M. A., and Madara, J. L. (1992) Neutrophil migration across a cultured epithelial monolayer elicits a biphasic resistance response representing sequential effects on transcellular and paracellular pathways. *J. Cell Biol.* **117**, 757–764
30. Chin, A. C., Fournier, B., Peatman, E. J., Reaves, T. A., Lee, W. Y., and Parkos, C. A. (2009) CD47 and TLR-2 cross-talk regulates neutrophil transmigration. *J. Immunol.* **183**, 5957–5963
31. Chakrabarti, S., and Patel, K. D. (2005) Regulation of matrix metalloproteinase-9 release from IL-8-stimulated human neutrophils. *J. Leukoc. Biol.* **78**, 279–288
32. Swamydas, M., and Lionakis, M. S. (2013) Isolation, purification and labeling of mouse bone marrow neutrophils for functional studies and adoptive transfer experiments. *J. Vis. Exp.* 77, e50586
33. Weber, D. A., Sumagin, R., McCall, I. C., Leoni, G., Neumann, P. A., Andargachew, R., Brazil, J. C., Medina-Contreras, O., Denning, T. L., Nusrat, A., and Parkos, C. A. (2014) Neutrophil-derived JAML inhibits repair of intestinal epithelial injury during acute inflammation. *Mucosal Immunol.* **7**, 1221–1232
34. Mayerle, J., Schnekenburger, J., Krüger, B., Kellermann, J., Ruthenbürger, M., Weiss, F. U., Nalli, A., Domschke, W., and Lerch, M. M. (2005) Extracellular cleavage of E-cadherin by leukocyte elastase during acute experimental pancreatitis in rats. *Gastroenterology* **129**, 1251–1267
35. Sumagin, R., Robin, A. Z., Nusrat, A., and Parkos, C. A. (2014) Transmigrated neutrophils in the intestinal lumen engage ICAM-1 to regulate the epithelial barrier and neutrophil recruitment. *Mucosal Immunol.* **7**, 905–915
36. Daniel, L., Fakhouri, F., Joly, D., Mouthon, L., Nusbaum, P., Grunfeld, J. P., Schifferli, J., Guillevin, L., Lesavre, P., and Halbwachs-Mecarelli, L. (2006) Increase of circulating neutrophil and platelet microparticles during acute vasculitis and hemodialysis. *Kidney Int.* **69**, 1416–1423
37. Kolaczkowska, E., and Kubes, P. (2013) Neutrophil recruitment and function in health and inflammation. *Nat. Rev. Immunol.* **13**, 159–175
38. Almkvist, J., Fäldt, J., Dahlgren, C., Leffler, H., and Karlsson, A. (2001) Lipopolysaccharide-induced gelatinase granule mobilization primes neutrophils for activation by galectin-3 and formylmethionyl-Leu-Phe. *Infect. Immun.* **69**, 832–837
39. Dalli, J., Norling, L. V., Renshaw, D., Cooper, D., Leung, K. Y., and Perretti, M. (2008) Annexin 1 mediates the rapid anti-inflammatory effects of neutrophil-derived microparticles. *Blood* **112**, 2512–2519
40. Jiang, K., Rankin, C. R., Nava, P., Sumagin, R., Kamekura, R., Stowell, S. R., Feng, M., Parkos, C. A., and Nusrat, A. (2014) Galectin-3 regulates desmoglein-2 and intestinal epithelial intercellular adhesion. *J. Biol. Chem.* **289**, 10510–10517
41. Corry, D. B., Kiss, A., Song, L. Z., Song, L., Xu, J., Lee, S. H., Werb, Z., and Kheradmand, F. (2004) Overlapping and independent contributions of MMP2 and MMP9 to lung allergic inflammatory cell egression through decreased CC chemokines. *FASEB J.* **18**, 995–997
42. Sumagin, R., Brazil, J. C., Nava, P., Nishio, H., Alam, A., Luissint, A. C., Weber, D. A., Neish, A. S., Nusrat, A., and Parkos, C. A. (2016) Neutrophil interactions with epithelial-expressed ICAM-1 enhances intestinal mucosal wound healing (E-pub ahead of print). *Mucosal Immunol.* 10.1038/mi.2015.135
43. Headland, S. E., Jones, H. R., Norling, L. V., Kim, A., Souza, P. R., Corsiero, E., Gil, C. D., Nerviani, A., Dell'Accio, F., Pitzalis, C., Oliani, S. M., Jan, L. Y., and Perretti, M. (2015) Neutrophil-derived microvesicles enter cartilage and protect the joint in inflammatory arthritis. *Sci. Transl. Med.* **7**, 315ra190

44. Chakrabarti, S., Zee, J. M., and Patel, K. D. (2006) Regulation of matrix metalloproteinase-9 (MMP-9) in TNF-stimulated neutrophils: novel pathways for tertiary granule release. *J. Leukoc. Biol.* **79**, 214–222
45. Erlandsen, S. L., Hasslen, S. R., and Nelson, R. D. (1993) Detection and spatial distribution of the beta 2 integrin (Mac-1) and L-selectin (LECAM-1) adherence receptors on human neutrophils by high-resolution field emission SEM. *J. Histochem. Cytochem.* **41**, 327–333
46. Gaborski, T. R., Sealander, M. N., Waugh, R. E., and McGrath, J. L. (2013) Dynamics of adhesion molecule domains on neutrophil membranes: surfing the dynamic cell topography. *Eur. Biophys. J.* **42**, 851–855
47. Kunder, C. A., St John, A. L., Li, G., Leong, K. W., Berwin, B., Staats, H. F., and Abraham, S. N. (2009) Mast cell-derived particles deliver peripheral signals to remote lymph nodes. *J. Exp. Med.* **206**, 2455–2467
48. Schulte, D., Küppers, V., Dartsch, N., Broermann, A., Li, H., Zarbock, A., Kamenyeva, O., Kiefer, F., Khandoga, A., Massberg, S., and Vestweber, D. (2011) Stabilizing the VE-cadherin-catenin complex blocks leukocyte extravasation and vascular permeability. *EMBO J.* **30**, 4157–4170
49. Wang, Q., and Doerschuk, C. M. (2001) The p38 mitogen-activated protein kinase mediates cytoskeletal remodeling in pulmonary microvascular endothelial cells upon intracellular adhesion molecule-1 ligation. *J. Immunol.* **166**, 6877–6884
50. Lu, P., Takai, K., Weaver, V. M., and Werb, Z. (2011) Extracellular matrix degradation and remodeling in development and disease. *Cold Spring Harb. Perspect. Biol.* **3**, 3
51. Pitanga, T. N., de Aragão França, L., Rocha, V. C., Meirelles, T., Borges, V. M., Gonçalves, M. S., Pontes-de-Carvalho, L. C., Noronha-Dutra, A. A., and dos-Santos, W. L. (2014) Neutrophil-derived microparticles induce myeloperoxidase-mediated damage of vascular endothelial cells. *BMC Cell Biol.* **15**, 21
52. Gasser, O., and Schifferli, J. A. (2004) Activated polymorphonuclear neutrophils disseminate anti-inflammatory microparticles by ectocytosis. *Blood* **104**, 2543–2548
53. Mackarel, A. J., Russell, K. J., Brady, C. S., FitzGerald, M. X., and O'Connor, C. M. (2000) Interleukin-8 and leukotriene-B(4), but not formylmethionyl leucylphenylalanine, stimulate CD18-independent migration of neutrophils across human pulmonary endothelial cells in vitro. *Am. J. Respir. Cell Mol. Biol.* **23**, 154–161
54. Pećina-Šand laus, N. (2003) Tumor suppressor gene E-cadherin and its role in normal and malignant cells. *Cancer Cell Int.* **3**, 17
55. Semb, H., and Christofori, G. (1998) The tumor-suppressor function of E-cadherin. *Am. J. Hum. Genet.* **63**, 1588–1593
56. Multhoff, G., Molls, M., and Radons, J. (2012) Chronic inflammation in cancer development. *Front. Immunol.* **2**, 98
57. Coussens, L. M., and Werb, Z. (2002) Inflammation and cancer. *Nature* **420**, 860–867

Received for publication June 13, 2016.
Accepted for publication August 8, 2016.